

Interactions between Ni and La₂O₃ in Ni/La₂O₃ Catalysts Prepared Using Different Ni Precursors

E. Ruckenstein¹ and Y. H. Hu²

Department of Chemical Engineering, State University of New York at Buffalo, Amherst, New York 14260

Received September 11, 1995; revised February 14, 1996; accepted March 1, 1996

The role of the anion (NO₃⁻ or Cl⁻), used in the preparation via impregnation of unreduced Ni/La₂O₃ catalysts, in the interactions between Ni and La₂O₃ was investigated using XRD, TPR, and ESCA experiments. The following results have been obtained: In the 20 wt% Ni/La₂O₃ prepared using Ni(NO₃)₂ as precursor, LaNiO₃ and La(OH)₃ were the only compounds identified by XRD in the sample calcined in O₂, and La₂NiO₄ and La(OH)₃ were the only compounds identified in the sample calcined in He. At lower Ni contents, the La₂O₃ phase was additionally identified. For the 20 wt% Ni/La₂O₃ prepared using Ni chloride as precursor, LaOCl was the only compound detected by XRD; no phase containing Ni was identified by XRD in the samples calcined in O₂ or He. At lower Ni chloride contents, LaNiO₃ was additionally detected in the sample calcined in O₂ and La₂NiO₄ in that calcined in He. A comparison between the XRD spectra and the TPR curves suggested the presence of amorphous NiO in the samples based on Ni chloride. It is also shown that the Ni precursor employed in the preparation of the catalyst plays a role in the CO₂ reforming of CH₄. During the CO₂ reforming of methane, the unreduced Ni/La₂O₃ catalysts, based on Ni nitrate, had a high initial CO yield but a low time stability; in contrast, the unreduced Ni/La₂O₃ catalysts, based on chloride, had a high stability. A possible explanation of this behavior, based on ESCA analysis and on the reaction between CH₄ and catalysts, is provided. © 1996 Academic Press, Inc.

INTRODUCTION

In the past few years it was found that the rare earth oxides, particularly La₂O₃, can improve the superconductive, optical, and catalytic properties of a variety of materials (1–9). The combination of rare earth oxides with transition metals generates the perovskite-type compounds ABO₃ (B, transition metal) (10–18), which can be used as catalysts. The various capabilities of the ABO₃ compounds are primarily due to the multiple valence states of the transition metals.

Nakamura *et al.* (10) studied the stability of LaBO₃ perovskites (B = V, Cr, Mn, Fe, Co, Ni). They found that, at

1273 K, LaNiO₃ decomposes into various compounds in various ranges of oxygen partial pressures. Crespin *et al.* (15) found that the low-temperature reduction of LaNiO₃ with hydrogen leads to new compounds, such as La₂Ni₂O₅ and LaNiO₂, before the complete reduction.

Even though numerous studies about the stability of oxides containing La and a transition metal have been carried out, no investigation regarding the effect of the anion present in the precursor employed in the preparation was yet performed. In the present paper, the effect of NO₃⁻ and Cl⁻ on the interaction between Ni and La₂O₃ was studied. We found that NO₃⁻, Cl⁻, and the gas atmosphere (O₂ or He) in which the thermal treatment occurs affect the phases formed from Ni and La₂O₃. The prepared catalysts have been employed to investigate the CH₄ decomposition as well as the CO₂ reforming of CH₄, and the results show that the Ni precursor affects the catalytic process.

1. EXPERIMENTAL

1.1. Catalyst preparation. The Ni/La₂O₃ catalyst was prepared by impregnating La₂O₃ powder (Aldrich, BET surface area of 2 m²/g) with a nickel nitrate or nickel chloride (Alfa) aqueous solution. The paste generated was dried at 110°C in air in an electric dryer for about 4 h, and then decomposed at 500°C for 4 h and calcined also for 4 h at 800°C in O₂ or He (20 ml/min) in an alumina reactor (6 mm inside diameter) located in a furnace. The composition and treatment conditions are listed in Table 1.

1.2. Temperature-programmed reduction (TPR). The TPR experiments were performed by heating the samples from room temperature to 800°C, at a rate of 17 K/min, in a 4% H₂/Ar gas flow rate of 47 ml/min through a quartz tube of 2 mm inside diameter. The temperature was measured with a thermocouple located in the catalyst bed. The produced gas was continuously detected with a thermal conductivity detector.

1.3. X-Ray powder diffraction and ESCA analysis. X-ray powder diffraction (XRD) was carried out using Nicolet X-ray diffraction equipment, equipped with a CuK α source, at 40 kV and 20 mA. The ESCA analysis

¹ To whom correspondence should be addressed.

² Permanent address: Department of Chemistry, Xiamen University, Xiamen 361005, P. R. China.

TABLE 1

Composition and Treatment Conditions of Samples

Sample No.	Ni content (wt%)	Calcination gas	Ni precursor
Ni-A-1	20	O ₂	Ni(NO ₃) ₂
Ni-A-2	20	He	Ni(NO ₃) ₂
Ni-A-3	10	O ₂	Ni(NO ₃) ₂
Ni-A-4	10	He	Ni(NO ₃) ₂
Ni-B-1	20	O ₂	NiCl ₂
Ni-B-2	20	He	NiCl ₂
Ni-B-3	10	O ₂	NiCl ₂
Ni-B-4	10	He	NiCl ₂

was carried out with a SSI Model 100 small spot ESCA instrument equipped with an AlK α monochromatized X-ray source.

1.4. CO₂ reforming of methane. The catalytic reaction was carried out under atmospheric pressure in a vertical quartz tube (2 mm inside diameter). The molar ratio of the reactant gases, with a GHSV of 60,000 cm³g⁻¹h⁻¹, was CO₂:CH₄ (1:1). The catalyst powder (weight, 0.020 g; bed height, 2 mm) was held on quartz wool. The system (the catalyst plus the flowing gases) was heated from 25 to 790°C in 35 min and maintained at 790°C for the remaining time of the experiment. The analysis of reactants/products mixtures was performed with an *in situ* gas chromatograph equipped with a Porapak Q column.

1.5. Pulse CH₄-MS response. A quartz tube (2 mm inside diameter) was used as a reactor. The catalyst powder (weight, 0.02 g; bed height, 2 mm) was held on quartz wool. The reactant CH₄ had a pulse volume of 45 μ l. Ultra-high purity helium was used as carrier gas, at atmospheric pressure and 600°C, with a flow rate of 60 ml/min (GHSV, 180,000 cm³g⁻¹h⁻¹). The analysis of gases during the transients was carried out with an on-line mass spectrometer (HP Quadrupole, 5971 series mass selective detector) equipped with a fast response inlet capillary system. The calibration of the mass spectrometer was performed with mixtures of known composition.

2. RESULTS

2.1. Analysis of the phases. Ni/La₂O₃ was prepared by impregnating La₂O₃ with NiCl₂ or Ni(NO₃)₂; this was followed by decomposition at 500°C and calcination at 800°C in O₂ or He (see Table 1). The XRD patterns showed that the phases generated depend on the precursor employed and calcining conditions. Figures 1 and 2 demonstrate that for the 20 wt% Ni/La₂O₃ catalysts prepared from Ni nitrate (Ni-A-1 and Ni-A-2), LaNiO₃ and La(OH)₃ are the only

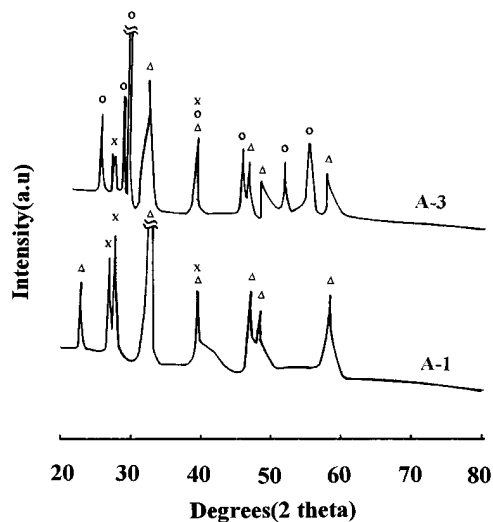


FIG. 1. X-ray powder diffraction spectra: (A-1), 20 wt% Ni/La₂O₃ (Ni-A-1), and (A-3), 10 wt% Ni/La₂O₃ (Ni-A-3), prepared from Ni nitrate and calcined in O₂ (Δ , LaNiO₃; \circ , La₂O₃; \times , La(OH)₃).

compounds present in Ni-A-1 (calcined in O₂), and La₂NiO₄ and La(OH)₃ are the only compounds present in Ni-A-2 (calcined in He). When the Ni content was decreased to 10 wt%, LaNiO₃, La(OH)₃, and La₂O₃ were identified in Ni-A-3 (calcined in O₂), and La₂NiO₄, La(OH)₃, and La₂O₃ were found in Ni-A-4 (calcined in He) (Figs. 1 and 2). For the 20 wt% Ni/La₂O₃ prepared from NiCl₂, LaOCl was the only compound identified both in Ni-B-1 and in Ni-B-2 (Figs. 3 and 4). However, when the Ni content was decreased to 10 wt%, besides LaOCl, LaNiO₃ was detected in Ni-B-3 (calcined in O₂) and La₂NiO₄ in Ni-B-4 (calcined in He)

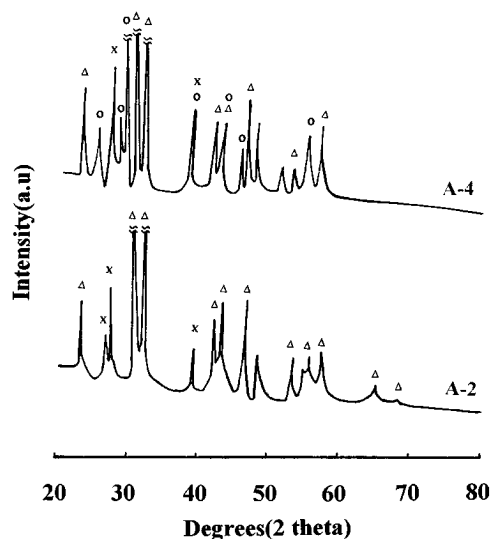


FIG. 2. X-ray powder diffraction spectra: (A-2), 20 wt% Ni/La₂O₃ (Ni-A-2), and (A-4), 10 wt% Ni/La₂O₃ (Ni-A-4), prepared from Ni nitrate and calcined in He (Δ , La₂NiO₄; \circ , La₂O₃; \times , La(OH)₃).

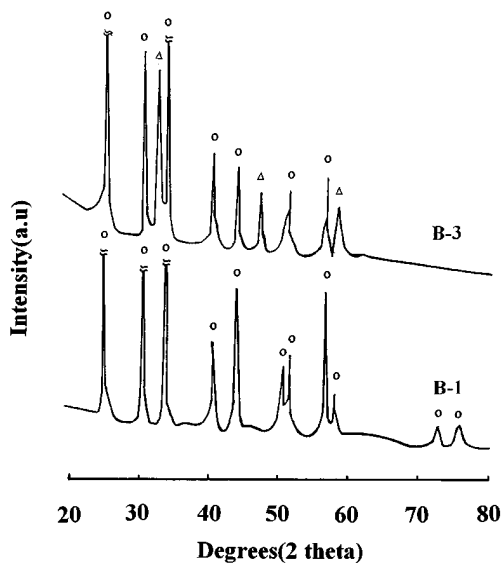


FIG. 3. X-ray powder diffraction spectra: (B-1), 20 wt% Ni/La₂O₃ (Ni-B-1), and (B-3), 10 wt% Ni/La₂O₃ (Ni-B-3), prepared from Ni chloride and calcined in O₂ (Δ, LaNiO₃; O, LaOCl).

(Figs. 3 and 4). The La(OH)₃, found in the nitrate-based catalysts, has its origin probably in the hydration of La₂O₃ in air, during manipulation of the catalysts.

2.2. Temperature-programmed reduction. As shown in Figs. 5 and 6, for the 20 wt% Ni/La₂O₃ catalysts prepared from Ni(NO₃)₂, there are two groups of overlapping peaks in the TPRs of Ni-A-1 and Ni-A-2. When the Ni content was decreased to 10 wt% (Ni-A-3 and Ni-A-4), the number of TPR peaks did not change; however, the height of the

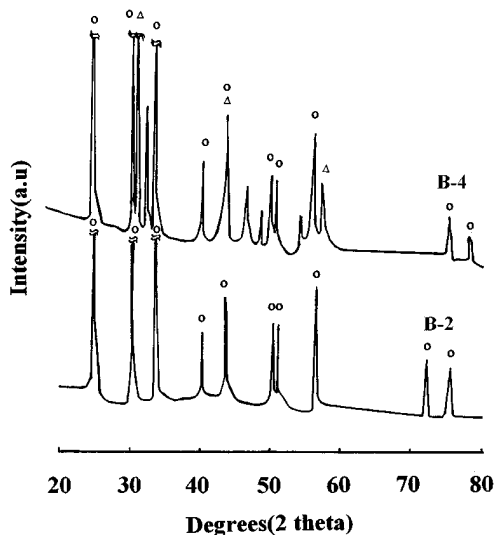


FIG. 4. X-ray powder diffraction spectra: (B-2), 20 wt% Ni/La₂O₃ (Ni-B-2), and (B-4), 10 wt% Ni/La₂O₃ (Ni-B-4), prepared from Ni chloride and calcined in He (Δ, La₂NiO₄; O, LaOCl).

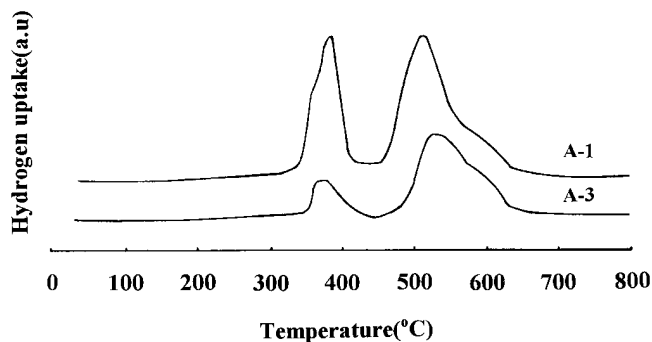


FIG. 5. Temperature-programmed reduction: (A-1), 20 wt% Ni/La₂O₃ (Ni-A-1), and (A-3), 10 wt% Ni/La₂O₃ (Ni-A-3), prepared from Ni nitrate and calcined in O₂.

lower temperature peak decreased (Figs. 5 and 6). For the 20 wt% Ni/La₂O₃ catalyst prepared from NiCl₂, only one peak was observed at 380°C in the TPR of Ni-B-1 (calcined in O₂) and in that of Ni-B-2 (calcined in He) (Figs. 7 and 8). Compared to the 20 wt% catalysts, the 10 wt% catalysts had very different TPR curves: besides the peak at about 400°C, two other peaks were observed at 510 and 580°C in Ni-B-3 (calcined in O₂), and a single peak was observed at 650°C for Ni-B-4 (calcined in He) (Figs. 7 and 8).

2.3. ESCA analysis. Table 2 presents the results of the surface analysis for three samples. It should be noted that the primary Ni peak (Ni 2p_{3/2}) overlaps with the La 3d_{3/2} peak. For this reason, the lower binding energy Ni 3p peak was scanned to ascertain if Ni was present; Ni was not detected on the surface of the three samples.

2.4. CO₂ reforming of methane. The results of the CO₂ reforming of methane showed that the 20 wt% Ni/La₂O₃ catalysts, prepared from Ni nitrate and calcined in either O₂ or He, had an initial CO yield of about 62%. However, because of the carbon deposition which followed, the reactor was completely plugged in 6 h. In contrast, the 20 wt%

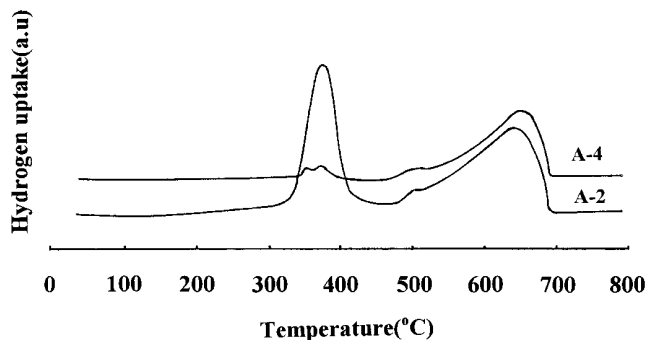


FIG. 6. Temperature-programmed reduction: (A-2), 20 wt% Ni/La₂O₃ (Ni-A-2), and (A-4), 10 wt% Ni/La₂O₃ (Ni-A-4), prepared from Ni nitrate and calcined in He.

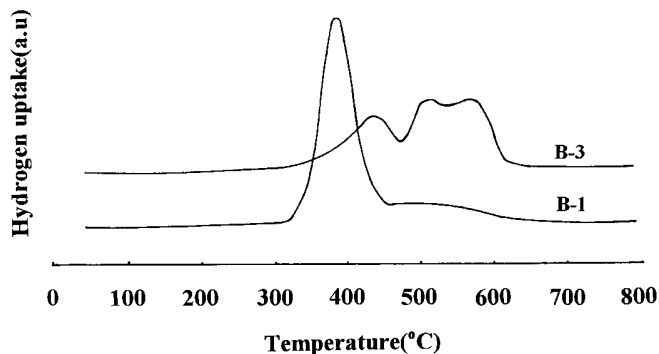


FIG. 7. Temperature-programmed reduction: (B-1), 20 wt% Ni/La₂O₃ (Ni-B-1), and (B-3), 10 wt% Ni/La₂O₃ (Ni-B-3), prepared from Ni chloride and calcined in O₂.

Ni/La₂O₃, prepared from Ni chloride, had high stability, the CO yield remaining at about 50% for 26 h (Fig. 9).

2.5. CO₂ and CO response of CH₄ pulse. The response experiments of CH₄ pulses showed that CO₂ is the main product and that a small amount of CO is generated over all fresh Ni/La₂O₃ catalysts. However, the intensity of the response of CO₂ was dependent on the Ni precursor and the treatment conditions employed (Figs. 10 and 11). The CO₂ intensity of the CH₄ pulse over Ni/La₂O₃ is much higher for the catalyst prepared from Ni(NO₃)₂ than from NiCl₂.

3. DISCUSSION

3.1. Phase composition. The XRD patterns show that different Ni precursors and treatment atmospheres result in different phases in the Ni/La₂O₃ catalyst. For Ni/La₂O₃ based on Ni nitrate, LaNiO₃ was the main phase, when the sample was calcined in O₂, and La₂NiO₄ was the main phase, when the sample was calcined in He (Figs. 1 and 2). Nakamura *et al.* noted that at the very high temperature of 1273 K, LaNiO₃ decomposes in a mixture of La₂NiO₄ and NiO for oxygen partial pressures in the

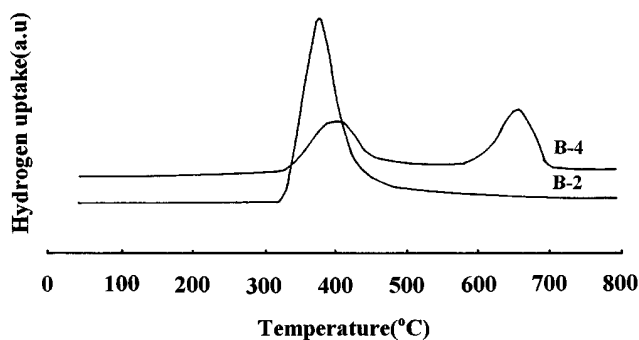


FIG. 8. Temperature-programmed reduction: (B-2), 20 wt% Ni/La₂O₃ (Ni-B-2), and (B-4), 10 wt% Ni/La₂O₃ (Ni-B-4), prepared from Ni chloride and calcined in He.

TABLE 2
Surface Composition of Ni/La₂O₃ Catalysts

Element	Ni-A-2	Ni-B-2	
		Before reaction	After reaction
Cl	—	38.4	11.6
O	83.5	47.9	83.6
La	16.5	13.7	4.8

range $10^{-2} > P_{O_2}(\text{Torr}) > 10^{-9}$ and a mixture of La₂NiO₄ and Ni⁰ in the range $10^{-9} > P_{O_2}(\text{Torr}) > 10^{-10}$ and that a complete decomposition into La₂O₃ and Ni⁰ occurs for $P_{O_2}(\text{Torr}) < 10^{-10}$. This indicates that a O₂-rich atmosphere favors the formation of the high valence Ni³⁺ and that LaNiO₃ is unstable in the absence of O₂. Different phases are formed when Ni/La₂O₃ is calcined in O₂ or He because the different calcining gases change the equilibrium between O₂ and the compounds containing Ni, La, and O. For the 20 wt% Ni/La₂O₃ prepared from Ni chloride, LaOCl was the only phase detected by XRD after calcination in either O₂ or He (Figs. 3 and 4). This indicates that Ni is present mostly in the amorphous state. When the nickel chloride content decreased, besides the LaOCl phase, the La₂NiO₄ phase was identified when the sample was calcined in He and the LaNiO₃ phase when the sample was calcined in O₂ (Figs. 3 and 4). This indicates that the reaction between Ni and La₂O₃ is affected not only by the partial pressure of O₂ but also by Cl⁻. When the Cl⁻ content is large enough Cl⁻ reacts with La₂O₃ and the reaction between Ni and La₂O₃ is inhibited, even at an O₂ pressure of 1 atm.

3.2. TPR curves. Each of the TPR curves of Ni/La₂O₃ prepared from Ni nitrate and calcined in O₂ or He exhibits two double-overlapped peaks (Figs. 5 and 6) one at 350 and 380°C and the other one at about 510 and about 600°C. The XRD pattern show that after the Ni/La₂O₃ catalyst

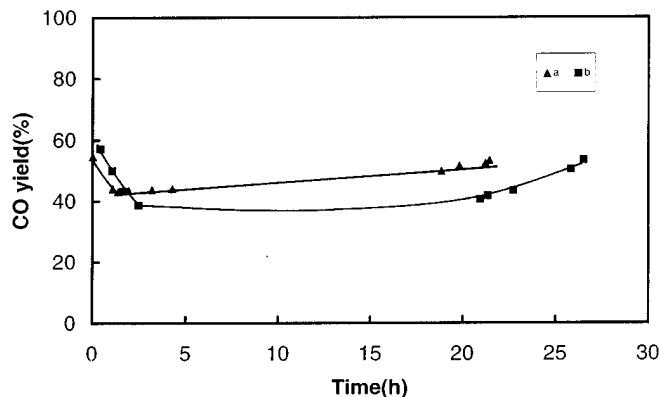


FIG. 9. CO yield vs reaction time for the unreduced 20 wt% Ni/La₂O₃ catalyst at 790°C: (a) Ni-B-1, (b) Ni-B-2.

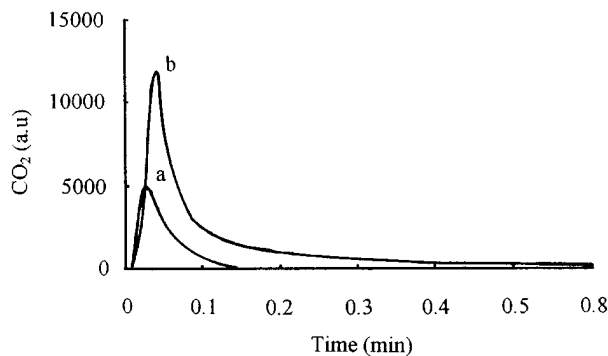


FIG. 10. MS-response curve of CO₂ from a CH₄ pulse over the 20 wt% Ni/La₂O₃ catalyst at 600°C: (a) Ni-B-1, (b) Ni-A-1.

based on Ni nitrate was reduced from room temperature to 450°C (which is below the high temperature peaks in the TPR curves), LaNiO₃ (for the sample calcined in O₂) and La₂NiO₄ (for the sample calcined in He) could still be detected (Fig. 12). This suggests that the low temperature peaks do not belong to LaNiO₃ and La₂NiO₄, but to the reduction of the amorphous Ni oxide. Consequently, it is reasonable to consider that the high temperature peaks are due to the reduction of LaNiO₃ and La₂NiO₄, respectively. For Ni-A-2 (calcined in He), the peak at about 600°C was the main one, while that at 510°C was very small (Fig. 6). Because the XRD pattern (Fig. 2) indicates that La₂NiO₄ constitutes the main phase, the peak at about 600°C should be attributed to the reduction of La₂NiO₄, while the lower peak at about 510°C might imply that a small amount of LaNiO₃ is also present, which was, however, too small to be detected by XRD. In contrast, in Ni-A-1 (calcined in O₂), the peak was higher at 510°C than at about 600°C (Fig. 5). The former peak can be attributed to LaNiO₃; the smaller peak at 600°C might be due to the partial reduction of La₂NiO₄ which is present in an amount too small to be detected by XRD. For the Ni-A-2 catalyst reduced in a TPR experiment up to 800°C, the XRD pattern shown that only

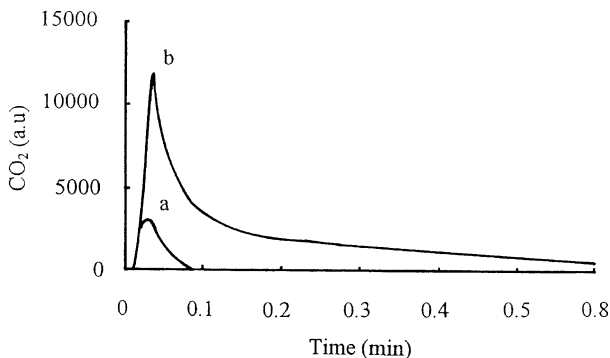


FIG. 11. MS-response curve of CO₂ from a CH₄ pulse over the 20 wt% Ni/La₂O₃ catalyst at 600°C: (a) Ni-B-2, (b) Ni-A-2.

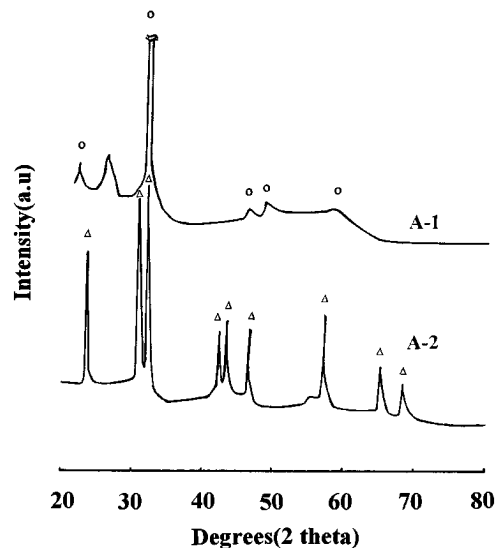


FIG. 12. X-ray powder diffraction spectra of the partially reduced 20 wt% Ni/La₂O₃ prepared from Ni nitrate. (A-1) Ni-A-1 and (A-2) Ni-A-2 were reduced with H₂ from room temperature to 450°C at a rate of 17°C/min (Δ, La₂NiO₄; ○, LaNiO₃).

La₂O₃ and Ni are present and that the other phases have been removed during the reduction process (Fig. 13).

The 20 wt% Ni/La₂O₃ prepared from Ni chloride has one peak at 380°C, which can be attributed to the reduction of the amorphous NiO (Figs. 7 and 8). Compared with pure NiO, which has a peak at 340°C (19), the peak temperature is higher, probably because NiO is dispersed into the crystalline LaOCl and this increases the difficulty of its reduction.

For the 10 wt% Ni/La₂O₃ prepared from Ni chloride, besides the peak at about 400°C, two overlapped peaks of comparable height were observed at 510 and 580°C in Ni-B-3 (calcined in O₂) and one single peak at 650°C in Ni-B-4 (calcined in He) (Figs. 7 and 8). The high temperature overlapped peaks are similar to those of LaNiO₃ or La₂NiO₄ in Ni/La₂O₃ prepared from Ni nitrate; hence they can be attributed to the presence of LaNiO₃ in Ni-B-3 and of La₂NiO₄ in Ni-B-4. This is consistent with the XRD results (Figs. 3 and 4).

Some quantitative information regarding the percentage of Ni in the amorphous and crystalline phases can be extracted from the TPR spectra and is presented in Table 3. Table 3 shows that the amount of amorphous Ni oxide is greater for the chloride based catalysts than for the corresponding nitrate based catalysts.

3.3. Activity and stability of catalysts for CO₂ reforming of CH₄. The CO yield remained almost unchanged over Ni-B-1 and Ni-B-2, prepared from NiCl₂, during the CO₂ reforming of CH₄, for 26 h (Fig. 9). In contrast, carbon deposition, which plugged the reactor was observed to occur over Ni-A-1 and Ni-A-2. The CO₂ response MS curves of

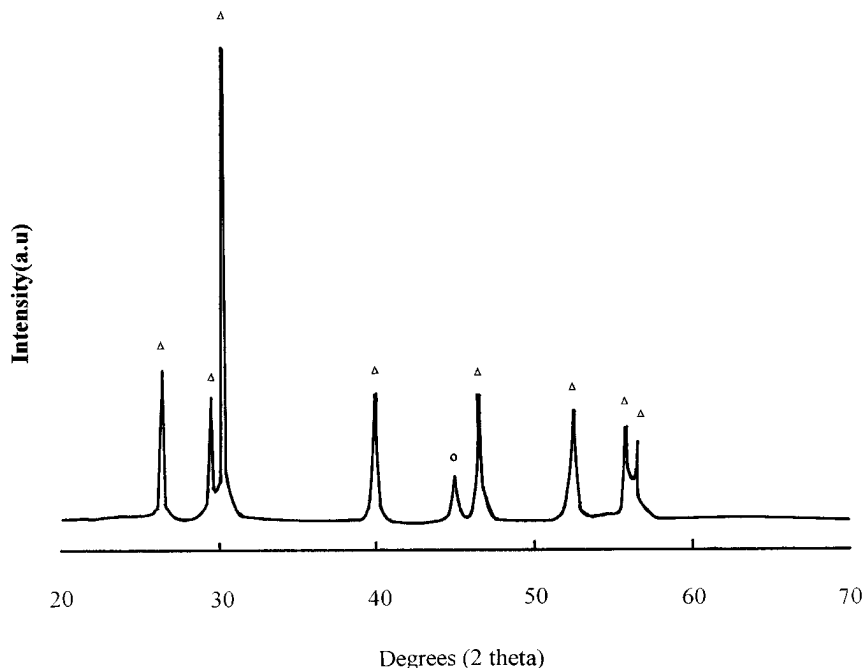


FIG. 13. X-ray powder diffraction spectra of the reduced 20 wt% Ni/La₂O₃ (Ni-A-2) prepared from Ni nitrate (The catalysts was reduced with H₂ from room temperature to 800°C at a rate of 17°C/min.) (Δ, La₂O₃; ○, Ni).

CH₄ pulses (Figs. 10 and 11) show that Ni-A-1 and Ni-A-2 were more easily reduced than Ni-B-1 and Ni-B-2. Therefore, a larger amount of Ni metal was generated by CH₄ during the CO₂/CH₄ flow over Ni-A-1 and Ni-A-2 than over Ni-B-1 and Ni-B-2. Because the Ni metal is the active site (19, 20), Ni-A-1 and Ni-A-2 have a higher initial CO yield than Ni-B-1 and Ni-B-2 in the CH₄/CO₂ reaction. However, a greater number of Ni metal sites results in a higher carbon deposition which leads to the plugging of the reactor. It is of interest to note (Fig. 14) that in the Ni-B-1 catalyst used in the CO₂ reforming of CH₄ at 790°C for 30 h, LaOCl, which was the only phase detected by XRD before reaction, was still present; (the monoclinic La₂O₃ could be also detected after reaction). Is the presence of LaOCl in the NiCl₂ based catalysts responsible for their higher sta-

bility? The ESCA experiments provide some information in this direction. The ESCA analysis could not detect Ni on the surface of both nitrate and chloride based catalysts. This means that its surface concentration is very small and that the surface is enriched in La in both cases. However, as already noted, the response to CH₄ pulses indicates a larger number of Ni sites on the nitrate based catalysts. In

TABLE 3

Content of Amorphous NiO in Ni/La₂O₃ Catalysts

Catalyst	Amorphous Ni oxide (mol%)
Ni-A-1	34
Ni-A-2	37
Ni-A-3	8
Ni-A-4	10
Ni-B-1	100
Ni-B-2	100
Ni-B-3	27
Ni-B-4	56

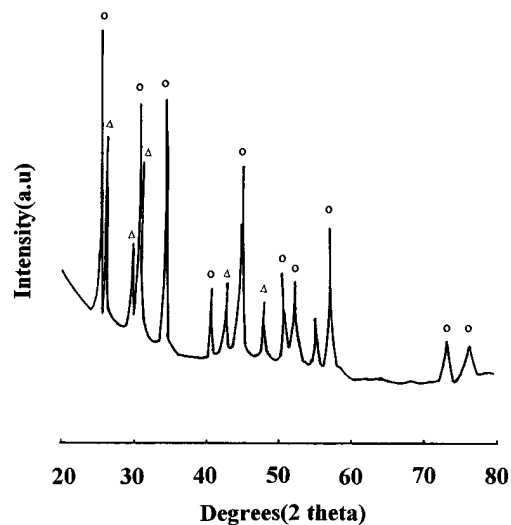


FIG. 14. X-ray powder diffraction spectra of the unreduced 20 wt% Ni/La₂O₃ prepared from Ni chloride and used in CO₂ reforming of CH₄ at 790°C for 4 h (Δ, La₂O₃; ○, LaOCl).

addition, Table 2 shows that the atomic ratio between Cl and La on the surface of the chloride based catalyst is almost the same before and after reaction. This suggests that a relatively stable compound containing Cl and La is present on the surface. The atomic ratio Cl/La for this compound is, however, larger than 1, the ratio in the compound LaOCl identified by XRD in the bulk both before and after reaction. Since the ESCA analysis provides a ratio near to 3, we are tempted to consider LaCl₃ as that compound, or another one, containing some oxygen in which the ratio Cl/La equals 3. That compound being surface active accumulates at the surface, but is present in the bulk in an amount too small to be detected by XRD. The number of Ni sites in the chloride based catalysts is smaller than in those based on nitrate because of the high surface activity of that compound. This impedes the formation of sufficiently large ensembles of Ni atoms which are necessary for coke deposition (21, 22).

4. CONCLUSION

The phase composition of the Ni/La₂O₃ catalyst depends on the nature of the Ni precursor used in the preparation and on the treatment conditions employed. This has catalytic implications, since in the CO₂ reforming of CH₄, the 20 wt% unreduced Ni/La₂O₃ catalyst prepared using Ni(NO₃)₂ as precursor has a low time stability, while the corresponding catalyst based on NiCl₂ has a high one. ESCA analysis and the reaction of the catalysts with CH₄ suggested a possible explanation for this behavior.

REFERENCES

1. Singh, P., and Kishore, R., *Superconductivity*, **8**(1), 9 (1995).
2. Sasai, H., Arai, T., Satow, Y., Houk, K. N., and Shibasaki, M., *J. Am. Chem. Soc.* **117**(23), 6194 (1995).
3. Hu, Y. H., and Ruckenstein, E., *J. Catal.* **158**, 260 (1996).
4. Ruckenstein, E., and Hu, Y. H., *Catal. Lett.* **35**, 265 (1995).
5. Hu, Y. H., and Ruckenstein, E., *Catal. Lett.* **34**, 41 (1995).
6. Deeba, M., Farrauto, R. J., and Lui, Y. K., *Appl. Catal.* **124**(2), 339 (1995).
7. Castro, F., and Nabet, B., *Appl. Opt.* **34**(13), 2317 (1995).
8. Tsubouchi, A., and Bruice, T. C., *J. Am. Chem. Soc.* **117**(28), 7399 (1995).
9. Horita, T., Choi, J. M., Lee, Y. K., Sakai, N., Kawada, T., Yokokawa, H., and Dokiya, M., *J. Am. Ceram. Soc.* **78**(7), 1729 (1995).
10. Nakamura, T., Petzow, G., and Gauckler, L. J., *Mater. Res. Bull.* **14**, 649 (1979).
11. Meadowcroft, D. B., Meier, P. G., and Warren, A. C., *Energy Convers.* **12**, 145 (1972).
12. Spacil, H. S., and Tedmon, C. S., *J. Electrochem. Soc.* **116**, 1618 (1969).
13. Libby, W. F., *Science* **171**, 499 (1971).
14. Gallagher, P. K., Johnson, D. W., and Vogel, E. M., *J. Am. Ceram. Soc.* **60**, 28 (1977).
15. Crespin, M., Gatineau, L., and Levitz, P., *J. Chem. Soc. Faraday Trans.* **2**(79), 1181 (1983).
16. Levitz, P., Crespin, M., and Gatineau, L., *J. Chem. Soc. Faraday Trans.* **2**(79), 1195 (1993).
17. Watson, P. R., and Somorjai, G. A., *J. Catal.* **74**, 282 (1982).
18. Tascon, J. M. D., Olivan, A. M. O., Tejuca, L. G., and Bell, A. T., *J. Phys. Chem.* **90**(5), 791 (1986).
19. Hu, Y. H., and Ruckenstein, E., *Catal. Lett.* **36**, 145 (1996).
20. Ruckenstein, E., and Hu, Y. H., *Appl. Catal.* **133**, 49 (1995).
21. Rostrup-Nielsen, J. R., *J. Catal.* **85**, 31 (1984).
22. Rostrup-Nielsen, J. R., *J. Catal.* **48**, 155 (1977).